

SIMS analysis of volatiles in silicate glasses

1. Calibration, matrix effects and comparisons with FTIR

Erik Hauri^{a,*}, Jianhua Wang^a, Jacqueline E. Dixon^b, Penelope L. King^{c,1},
Charles Mandeville^d, Sally Newman^e

^aDepartment of Terrestrial Magnetism, Carnegie Institution of Washington, 5241 Broad Branch Rd. NW, Washington, DC 20015, USA

^bDivision of Marine Geology and Geophysics, Rosenstiel School of Marine and Atmospheric Science, University of Miami, Coral Gables, FL 33149, USA

^cDepartment of Geological Sciences, Arizona State University, Tempe, AZ 85287, USA

^dAmerican Museum of Natural History, Central Park West at 79th St., New York, NY 10024, USA

^eDivision of Geological and Planetary Sciences, California Institute of Technology, Pasadena, CA 91125, USA

Received 30 November 1999; accepted 2 May 2001

Abstract

This paper describes microanalysis techniques using secondary ion mass spectrometry (SIMS) to measure the abundances and isotopic compositions of hydrogen, carbon, fluorine, sulfur and chlorine in volcanic glasses. SIMS measurement of total H₂O and total CO₂ abundances compare very well with measurements on the same glasses using vibrational spectroscopy techniques (FTIR). A typical 10-min SIMS measurement for volatile abundances is made on a singly polished specimen, sputtering a crater 15–30 μm in diameter and 2–3 μm deep, utilizing 1–5 × 10⁻⁹ g of sample material. Detection limits are routinely <30 ppm H₂O, <3 ppm CO₂, and <1 ppm F, S and Cl. Measurements of δD, δ¹³C and δ³⁴S in volcanic glasses are currently reproducible and accurate to 2–5‰, depending on the concentration of the element. Because of their spatial selectivity, the SIMS methods allow resolution of magmatic volatile signatures from those carried by secondary phases, which can sometimes plague traditional vacuum extraction methods that require large amounts of sample (tens to hundreds of milligrams). Ease of sample preparation, rapid analysis and high sensitivity allow SIMS to be applied to volatile analysis of small samples such as melt inclusions, in which large numbers of individual analyses are often required in order to obtain a representative sample population. Combined abundance and isotopic composition data for volatile elements provide coupled constraints on processes relevant to magma genesis and evolution, including degassing, magma contamination, mixing, and source variability. © 2002 Elsevier Science B.V. All rights reserved.

Keywords: SIMS; Ion probe; Volatiles; Microbeam; Water; Isotopes

1. Introduction

Measurements of volatile species such as H₂O, CO₂, F, S and Cl often rely on bulk rock analysis techniques which utilize vacuum extraction combined with either manometry or mass spectrometry (see

* Corresponding author. Fax: +1-202-478-88211.

E-mail address: hauri@dtm.ciw.edu (E. Hauri).

¹ Present address: Department of Earth Sciences, University of Western Ontario, London ON N6A 5B7, UK.

review by Ihinger et al., 1994). In the analysis of volcanic glasses with low volatile abundances, when a primary magmatic signature is desired, bulk extraction techniques can sometimes suffer from problems associated with the large amounts of material (up to several hundred milligrams) required for accurate measurements. Even with careful handpicking, bulk analyses of such large amounts of material can be compromised by contamination associated with adsorbed volatiles and minute amounts of altered material, and place sample size limitations on the types of studies which can be undertaken. In principal, a microbeam technique with sufficient sensitivity to measure low volatile abundances could circumvent these problems.

Within the last 25 years, electron microprobes have been modified to allow direct and indirect (in the case of water) microanalysis of volatile elements, but the high detection limits of this technique (tens to hundreds of ppm) place limitations on many volatile studies (cf. Devine et al., 1995 and references therein). Microanalysis techniques based on vibrational spectroscopy (such as Fourier Transform Infrared spectroscopy, FTIR) and secondary ion mass spectrometry (SIMS) have permitted the direct measurement of a number of volatile elements in silicate glasses, along with fine-scale spatial resolution which can be used to avoid contributions from secondary phases. The past decade has seen a rapid increase in the use of FTIR to measure quantitatively the abundance of a number of hydrogen- and carbon-bearing species in geological samples (Stolper, 1982; Fine and Stolper, 1986; Newman et al., 1986; Dixon et al., 1988; Fogel, 1989; Michael, 1995; Zhang et al., 1997; Wallace and Anderson, 1998; King, 1999). This technique combines a number of attractive improvements over bulk extraction and electron beam methods, which include a non-destructive analysis, the ability for microanalysis (down to 10–20 μm) and low detection limits (single ppm range), and the important ability to measure quantitatively the abundance of several H- and C-bearing species (H_2O , OH^- , CO_2 , CO_3^-). These advantages have facilitated improved experimental studies of volatile behavior in magmatic systems (Stolper and Holloway, 1988; Silver et al., 1990; Zhang and Stolper, 1991; Dixon and Stolper, 1995), with resulting benefits in understanding volatile behavior in natural samples. Disadvantages of this

technique include a laborious double-polishing sample preparation and the requirement of sufficient sample thickness to allow precise absorbance measurements. Some sample preparation problems are circumvented by reflectance FTIR (Grzechnik et al., 1996), but development efforts with both IR techniques have revealed significant matrix effects (Dixon and Pan, 1995; Zhang et al., 1997; King, 1999).

Most of these disadvantages are circumvented by ion probe analysis with some success (Delaney and Karsten, 1981; Hervig, 1992; Sisson and Layne, 1993; Deloule et al., 1995; Sobolev and Chaussidon, 1996). However, beginning with the first SIMS measurements of volatile contents (Hinthorne and Anderson, 1975), historically the ion probe techniques have suffered from high backgrounds and poor detection limits, particularly for H_2O and CO_2 (Ihinger et al., 1994; Devine et al., 1995). In this paper we describe new improvements in secondary ion mass spectrometry which permit the rapid analysis of the volatile elements H, C, F, S and Cl at the 5–10 μm scale in standard singly polished samples (e.g. thin sections, grain mounts) with greatly improved detection limits. In this paper we describe in detail our methods for minimizing these problems, discuss the overall technique and its calibration against high-quality FTIR measurements, outline methods for SIMS isotopic analysis of H, C and S in volcanic glasses, and apply the SIMS techniques to the study of volatile elements in olivine-hosted melt inclusions from several Hawaiian volcanoes (Hauri, 2001).

2. Standards and cross-calibration

We have utilized a number of natural and synthetic glass samples, ranging from nephelinite to rhyolite, to construct a SIMS calibration for the analysis of H, C, F, S and Cl abundances, and the isotopic compositions of H, C and S (Table 1). Many of these glasses have previously been analyzed for H_2O and CO_2 abundances by vacuum extraction manometry to provide a calibration for FTIR absorbance measurements. Most of the remaining glasses have been analyzed by FTIR using the most current absorbance calibrations, taking into account matrix effects on IR absorbance (Dixon and Pan, 1995; Zhang et al., 1997; King, 1999). SIMS calibrations for S and Cl abundances are based on

Table 1
Volatile abundances of SIMS silicate glass standards

Standard name	H ₂ O, wt.%	CO ₂ , ppm	F, ppm	S, ppm	Cl, ppm	References
<i>Basaltic</i>						
1833-1	2.430	24			800	1
1833-11	1.200	102			300	1
1846-12	1.550	90			380	1
WOK-28-3	0.500	183			80	1
30-2	0.600					4
40-2	0.150					4
519-4-1	0.170	165		1020		5
526-1	0.250			950		6
Bouvet	0.520					6
SLNT	0.490					6
IOC-1	0.240					6
3048-7		807				7
3048-11		24,270				7
3048-13		21,780				7
3048-15		17,270				7
3048-16		11,770				7
KK 15-5	0.780	92		1050	650	2
KK 16-1	0.500	45		1300	240	2
KK 17-17	0.470			1490	800	2
KK 18-8	0.600	47	600	2100	840	2,3
KK 20-14	0.480			1580	800	2
KK 23-3	0.440	32	400	1370	410	2,3
KK 24-13	0.580			1730	355	2
KK 26-5	0.560	111		1520	870	2
KK 27-3	0.460	61		1810	940	2
KK 27-14	0.600	108		1340	690	2
KK 27-19	0.530	60		2150	1100	2
KK 29-3	0.480	44		1770	640	2
KK 29-10	0.380	44		1250	390	2
KK 31-12	0.670	92		1070	300	2
NA 23-6	0.980	800		1380	1070	2
NA 24-3	0.930	600		1200	970	2
NA 27-2	0.830	630		1220	1150	2
NA 9-5	0.910	390		1370	850	2
NA 22-5	0.690	260		1390	450	2
<i>Andesitic</i>						
Run #9	3.740					8
Run #10	5.050					8
Run #12	3.740					8
MHA-23	0.760					9
MHA-25	1.850					9
MHA-26	2.430					9
MHA-27	0.850					9
MHA-30	2.480	1900				9
MHA-31	1.090	1900				9
MHA-41	2.690	4500				9
MHA-44	3.700					9
Blank	0.001					9

(continued on next page)

Table 1 (continued)

Standard name	H ₂ O, wt.%	CO ₂ , ppm	F, ppm	S, ppm	Cl, ppm	References
<i>Silicic</i>						
MC84-t	0.793	5				^a
MC84-df	0.707	7				^a
North Coulee	0.101					^a
NW Coulee	0.297					^a
Panum Dome	0.120	1				^a
UA 1113	2.800					11
UA 1112	4.800					11
Lipari	0.400					^a
Ab1	1.740	224				^a
UA 1162	6.380	7				^a
UA 1170	2.920	342				^a
UA 1115	0.660					^a
DC-1	0.238					^a
DC-2	0.127					^a
NC5-V	0.798					^a
BGM-8	0.386					^a
GML	0.120					6
NOR	6.050					^a
CO ₂ -1 blank	0.137	< 10				12
147	0.192	2860				12
149	0.107	1790				12
152	0.112	950				12
NBS 610			295	500	500	13,14
NBS 612			50	50	50	14
NBS 620				1120		14

(1) Stolper and Newman, 1994; Newman et al., 2000.

(2) Dixon and Clague, 2001.

(3) Byers et al., 1985.

(4) A. Sobolev, unpublished data.

(5) Fine and Stolper, 1986.

(6) Stolper, 1982.

(7) Dixon and Pan, 1995.

(8) Mandeville, unpublished data.

(9) King, unpublished data.

(10) Newman et al., 1988.

(11) Virgo, unpublished data.

(12) Fogel and Rutherford, 1990.

(13) Hoskin, 1999.

(14) Nominal and certified NIST values.

^a This study.

high-quality electron microprobe measurements of these elements in many of the same standards which have been analyzed by FTIR for H₂O and CO₂ (Dixon et al., 1997; Dixon and Clague, 2001).

Dissolved water concentration were analyzed on a Brüker IFS-66 infrared spectrometer at the University of Miami. Spectra were collected using an infrared microscope attachment, a Globar source, KBr beamsplitter and a HgCdTe₂ detector for the infrared region

and the main sample chamber, a W source, CaF₂ beamsplitter and an InSb detector for the near-infrared region. Glasses were double polished to a thickness of 50–300 μm. Thicknesses were measured using a digital micrometer to ± 2 μm. Reported water concentrations are the sum of molecular H₂O (5230 cm⁻¹ band) and hydroxyl group (4500 cm⁻¹) concentrations calculated from measured absorbances using densities reported in the literature (Stolper,

1982; Newman et al., 1986; Silver et al., 1990) and, for rhyolitic glasses, the method of Zhang et al. (1997) which allows the molar absorptivities to vary as a function of the total water content. Total water concentrations were also determined using the 3550 cm^{-1} absorption on both infrared and near-infrared spectra for rhyolitic glasses having less than about 0.7 wt.% H_2O .

Most of the rhyolitic glasses common to this study and those of Stolper (1982) and Newman et al. (1986) have been remeasured, and most of the new water concentrations are within 5% of the amounts determined by manometry with the exceptions of DC1 (16% lower), NC5V (11% higher) and North Coulee (2.5 times lower). Differences of our values from those determined by manometry may be related to sample heterogeneity. For the rhyolitic glasses, the mean water content determined from the 3550 cm^{-1} band and using a molar absorptivity of $90\text{ l mol}^{-1}\text{ cm}^{-1}$ are within 8% of the reported values. Previously published values of ϵ^{3550} for rhyolitic glasses of $100\text{ l mol}^{-1}\text{ cm}^{-1}$ (Newman et al., 1986) and $80\text{ l mol}^{-1}\text{ cm}^{-1}$ (Ihinger et al., 1994) result in total water concentrations that are 11% lower and higher, respectively, than our reported values.

Carbon dissolved as carbonate in basaltic glasses was determined using methods and absorbances described by Dixon and Pan (1995). Carbon dissolved as molecular CO_2 in the albitic glasses was measured using the 2350 cm^{-1} absorption in both near-IR (NIR) and mid-IR (MIR) spectra and a molar absorptivity of $945\text{ l mol}^{-1}\text{ cm}^{-1}$ (Fine and Stolper, 1985). Carbon dissolved as carbonate groups in the albite glasses was difficult to measure because of the overlap of the molecular water (1630 cm^{-1}) and carbonate (1610 and 1375 cm^{-1}) bands. We estimated the amount of carbonate in these glasses by assuming constant proportions of carbonate and molecular carbon dioxide ($\text{CO}_3^{2-} = 1.43\text{ CO}_2$ molecular) as determined for albitic glasses by Fine and Stolper (1985). Reported total CO_2 concentrations are the sum of the measured molecular CO_2 and estimated CO_3^{2-} concentrations.

All of the standards listed in Table 1 were used to construct the SIMS calibration curves. In most cases, FTIR and SIMS analyses were performed on the same spot on the same chip of glass. SIMS calibrations for S and Cl abundances are based on high-quality

electron probe measurements of these elements in many of the same standards which have been analyzed by FTIR for H_2O and CO_2 . Table 1 provides the sample numbers, concentrations, references, and analytical comments for each of the standards used in the SIMS calibrations.

3. Ion microprobe methods

3.1. Sample preparation for SIMS

The quality of the vacuum inside the ion microprobe sample chamber is the dominant factor which controls the background for H_2O and D/H measurements, and epoxy from sample mounts is the largest detractor to the mass spectrometer vacuum. In order to control the H background, the standards were mounted in one of two ways. Irregularly shaped glass fragments were mounted in epoxy in Al-metal disks and polished, or were first polished and pressed into indium metal. Doubly polished wafers prepared for FTIR were cleaned with methanol and mounted with super-glue directly onto the polished and cleaned surface of an Al-metal disk. All mounts were dried in an oven at $70\text{ }^\circ\text{C}$ for several days before coating with gold (both top and sides) for ion probe analysis. Between ion probe sessions, all standards (and samples) are stored in an oven at $70\text{ }^\circ\text{C}$ so as to minimize the adsorption of water vapor from laboratory air.

3.2. Volatile abundance measurements

The Cameca IMS 6f ion microprobe at the Department of Terrestrial Magnetism was used for all of the SIMS measurements. Prior to measurements, samples and standards are allowed to outgas in an airlock attached to the ion microprobe sample chamber, until pressures reached $<5 \times 10^{-8}$ Torr. Sample mounts outgas further once they are inserted into the sample chamber, and analyses are not begun until the sample chamber pressure has reached $<5 \times 10^{-9}$ Torr without the use of a cold finger. It is usually possible to obtain measurements at total sample chamber pressures $<10^{-9}$ Torr.

The major improvements over previous ion probe techniques are the high-quality vacuum and the use of a Cs^+ primary beam with collection of negatively

charged secondary ions. The primary beam (5–10 nA) is accelerated to 10 kV, tuned using Kohler illumination of a 100- μm diameter aperture, and slightly defocused to obtain a 20–40- μm diameter spot with a homogeneous intensity, resulting in a flat-bottomed sputter crater. Tuning of the primary beam is made with the mass spectrometer at low mass resolution, at a mass resolving power (MRP) of 300.

Due to implantation of Cs^+ ions and extraction of both negatively charged secondary ions and electrons, positive charging of the sample surface must be compensated with the use of an electron flood gun which delivers electrons to the sample surface. Tuning of the electron gun is made with the mass spectrometer at low mass resolution (MRP=300) and the energy slit wide open. During analysis, the sample potential is held at -5 kV and the electron gun is operated at -5 kV, so that electrons arrive at the sample surface with near-zero energy. Tuning of the intensity and density of the electron gun prior to each analysis session is achieved by offsetting the sample voltage by $+20$ V, allowing electrons to impact a conductive sample surface (Cu–Al grid) and viewing an image of H^- ions desorbed from the sample surface. The image of desorbed H^- ions defines the impact area of the electron beam, and the electron beam is tuned to deliver at least 40 μA of electron current (at 20 eV impact energy) homogeneously distributed over a 150 - μm diameter area. Final adjustments in the position and tuning of the electron beam are made by returning the sample potential to -5 kV, sputtering a gold-coated insulating sample (silicate glass) with the primary beam, and examining the images of H, O and Si with a narrow energy slit (± 2 – 3 eV). Particular attention is paid to achieving a homogeneous spot image (indicating homogeneity of charge compensation) and precise spatial coincidence of H, O and Si images. Finally, the filament current of the electron flood gun is decreased to an electron emission current well in excess of that required for charge compensation of a 20 nA Cs^+ primary beam (typically 200 – 300 nA). This “minimalist” electron current reduces the instrumental H background derived from electron sputtering along the electron beam path inside the machine, and provides the best possible sharpness of the secondary ion extraction optics and ion image of the sputtered sample surface while still maintaining effective charge compensation.

For analysis of H, C, F, S and Cl abundances, the mass spectrometer is tuned with an imaged field of view of 150 μm diameter on the sample surface, using a large contrast aperture at the crossover (400 μm). A 100 - μm diameter field aperture is inserted into the image plane, and entrance and exit slits are then closed to achieve a mass resolution of 2400, sufficient to resolve ^{18}OH from ^{19}F and $^{16}\text{O}_2$ from ^{32}S . The use of the 100 - μm field aperture is important; when properly aligned with the sputter crater, it limits the ion optical field of view to an area 10 μm in diameter (e.g. smaller than the primary beam diameter) and admits into the mass spectrometer only those ions originating from the central 10 μm of the crater. The elimination of stray ions sputtered from the crater walls and desorbed from the sample surface results in very low volatile backgrounds, particularly for hydrogen. The lack of charging is confirmed to within a few eV by checking manually the centering of a nearly closed energy slit on the peak of the Si energy distribution. Analyses are made with the energy slit wide open (250 eV bandpass).

Negatively charged secondary ions were counted by a Pulse Count Technologies ECL counting system (deadtime 11 ns), counting for 10 s on ^1H , ^{12}C , ^{19}F , ^{32}S and ^{35}Cl , and 2 s on the normalizing isotope ^{30}Si . The counting system background is <5 counts per minute for the counting system at half-mass positions with the primary beam and electron gun on. A single measurement consists of a 5-min presputter period with subsequent collection of five sets of ratios; the total analysis time is 10 min per spot. The depth of the sputter crater varies from 1 to 3 μm depending on primary beam intensity. Even using a small field aperture, useful ion yields are quite high for the elements of interest (H = 1 cps/ppm $\text{H}_2\text{O}/\text{nA}$; C = 0.4 cps/ppm/nA; F = 50 cps/ppm/nA; S = 10 cps/ppm/nA; Cl = 16 cps/ppm/nA). Detection limits were determined by analysis of San Carlos olivine, using literature estimates for concentrations of H_2O (10 ppm, Mackwell and Kohlstedt, 1990) and C (<2 ppm, Mathez and Delaney, 1981). Routine detection limits are <10 – 30 ppm H_2O , <3 ppm CO_2 , and <1 ppm F, S and Cl. These low detection limits are made possible by a combination of factors, dominated by (1) the high-quality vacuum, (2) the high useful yield of negative ions of these elements when using a Cs^+ beam, (3) the use of a small field aperture which

masks ion emission from outside the center of the sputter crater, and (4) low total electron current from the electron gun used for charge compensation.

3.3. Isotopic measurements by SIMS

Methods for D/H measurements will be described in detail in an upcoming paper (Hauri et al., in preparation); only a brief description will be given here. The mass spectrometer is operated at low mass

resolution (MRP=300). Under good vacuum conditions in the ion probe sample chamber ($<5 \times 10^{-9}$ Torr), repeated measurements of the H₂/D ratio in volcanic glasses demonstrate that this ratio is always $<1.5 \times 10^{-3}$ in glasses ranging from 0.1 to 5.6 wt.% H₂O, permitting δ D measurements at the 2–3 ‰ level at low mass resolution without hydride corrections. In order to maximize the instrument sensitivity for H, a larger field aperture is used (400 μ m) in combination with a smaller image field (100 μ m), and the primary

Table 2
Glass standards for hydrogen, carbon and sulfur isotope analysis

Standard name	H ₂ O, wt.%	δ D, ‰	C, ppm	δ^{13} C, ‰	S, ppm	δ^{34} S, ‰	References
<i>Basaltic</i>							
GL07 D30-1	1.54	–40					1
GL07 D52-5	1.00	–51					1
GL07 D53-2	0.77	–54					1
MK1-2	0.56	–78					2
GL07 D51-3	0.44	–52					1
KK29-10	0.38	–74					3
EN113 20D-1	0.25	–75					1
EN113 35D-1	0.16	–44					1
EN113 46D-2	0.11	–65					1
SAV-C-1			7000	–8.0			^a
ALV981-R23			406	–5.7			4
ALV519-4-1					980	1.6	^a
<i>Andesitic</i>							
Run58a	5.68	–244					^a
Run58b	4.45	–201					^a
Run9	4.35	–47					^a
MHA-44	3.70	–76	1300	–29.0			5
MHA-41	2.69	–83	920	–28.0			5
MHA-30	2.48	–63	270	–27.0			5
MHA-25	1.85	–62					5
MHA-31	1.09	–81	270	–27.0			5
<i>Silicic</i>							
#71	4.53	–118					6
#18	2.35	–140					6
GB37	1.14	–133					6
MC 84-t	0.79	–75					7
MC 84-df	0.70	–69					7
NWCoulee	0.30	–104					7
Panum Dome	0.12	–123					7

(1) Dixon and Kingsley, unpublished data.

(2) Garcia et al., 1989.

(3) Rison and Craig, 1983.

(4) Macpherson et al., 1999.

(5) King, unpublished data.

(6) Hervig, personal communication.

(7) Newman et al., 1988.

^a This study.

beam is further defocused so that ions from the outer 10 μm of the sputter crater are not admitted into the mass spectrometer.

The D/H measurements rely on several natural and synthetic glasses of basaltic, andesitic and rhyolitic compositions with known compositions and D/H ratios (Table 2). All of these glasses show excellent agreement between water determinations by FTIR and the manometric methods used during D/H analysis via bulk extraction. Negatively charged H and D ions are counted at low mass resolution (MRP=300) and full transmission using an ETP multiplier and an ECL counting system (11–14 ns deadtime) at count rates up to 2 MHz for H. These high H count rates do not result in short-term degradation of the EM gain because the low secondary electron yield of H on the first dynode of the multiplier (i.e. quantum efficiency) does not result in the high fluxes of secondary electrons at the end of the EM dynode chain typical of heavier isotopes at similar count rates. At these count rates, drift in the D/H instrumental mass fractionation (IMF) is usually $< 5\%$ per day.

A typical SIMS D/H analysis requires 20–40 min to reach 2–3‰ precision (1σ), limited only by counting statistics on D. The reproducibility of repeat measurements is identical to counting statistics for samples with $\text{H}_2\text{O} \geq 0.5$ wt.%, but is sometimes worse for samples with lower water contents (± 4 – 6% 1σ), particularly among the rhyolite glasses. In practice, from sample to sample, the primary beam intensity is adjusted in order to maintain a count rate of 1 – 2×10^6 cps on H, such that samples with 0.1 wt.% H_2O require a beam intensity of about 10–15 nA. The poorer reproducibility on some (but not all) low- H_2O glasses may be indicative of sample heterogeneity.

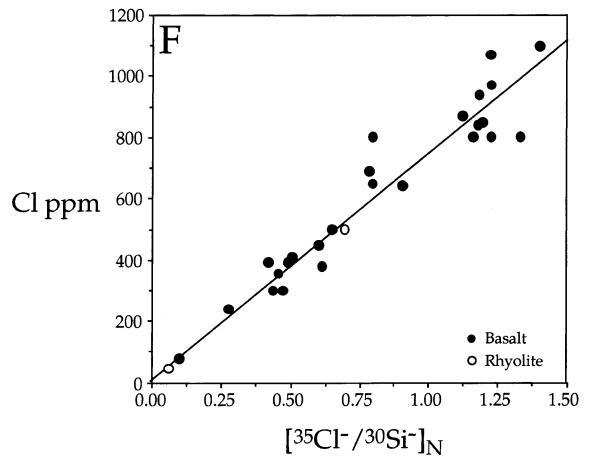
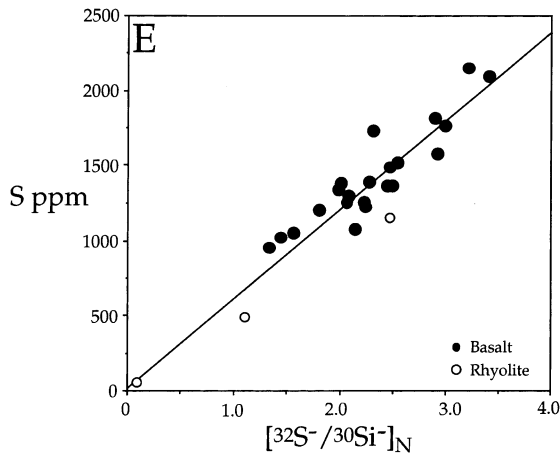
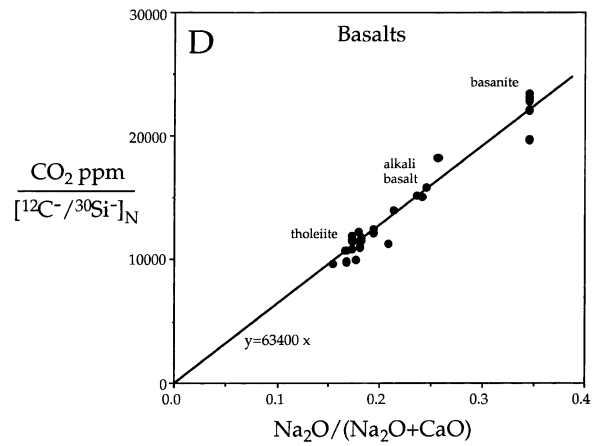
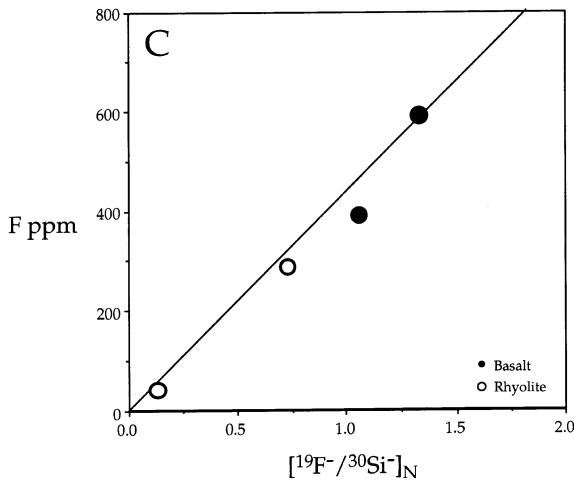
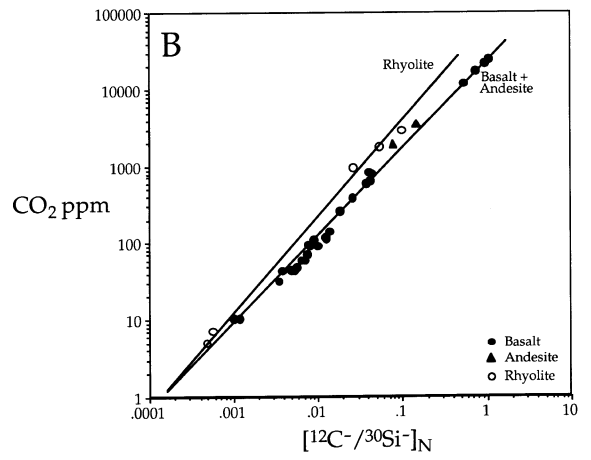
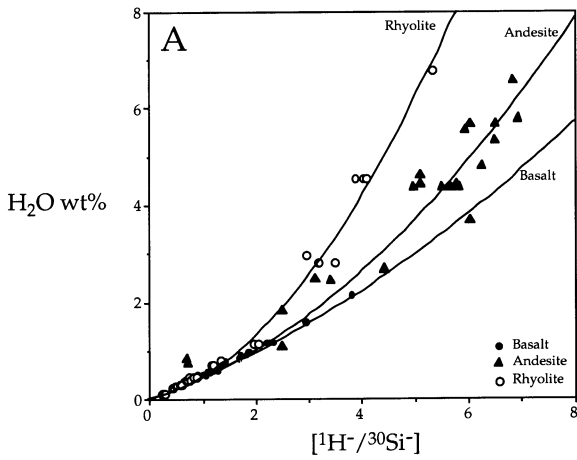
For analysis of C and S isotopes, the mass resolution is increased to 3200 to eliminate several interferences: ^{12}CH on ^{13}C , $^{16}\text{O}_2$ on ^{32}S , and ^{33}SH and $^{17}\text{O}_2$ on ^{34}S . The isotopic standards for $\delta^{13}\text{C}$ include several andesite glasses and two basalts, one of which is a natural glass (ALV981-R23 from Macpherson et

al., 1999). The other basalt glass is a synthetic sub-aerial basalt from Samoa which was doped with Iceland Spar calcite ($\delta^{13}\text{C} = -8.0 \pm 0.1\%$, 2σ) and synthesized to a glass at a P – T condition (10 kbar–1400 °C) which assures that the melt remained under-saturated with CO_2 . The resulting CO_2 concentration measured by SIMS is 7000 ppm. The isotopic standard for $\delta^{34}\text{S}$ is a sulfide-saturated MORB glass (ALV 519-4-1 from FAMOUS) in which dissolved sulfur is assumed to be isotopically identical to the $\delta^{34}\text{S}$ of co-existing immiscible sulfides ($+1.6 \pm 1.0\%$, 2σ). Typical precision and reproducibility on $\delta^{13}\text{C}$ and $\delta^{34}\text{S}$ depend upon the elemental concentrations, but is usually in the range of 2–4‰ for a 30–60 min analysis at 100–2000 ppm levels of CO_2 and S.

4. Calibration, matrix effects and accuracy

The SIMS calibration curves for H_2O , CO_2 , F, S and Cl are shown in Fig. 1. The calibrations for H_2O are linear up to 1.5 wt.% H_2O , with basalts, andesites and rhyolites describing a single line (Fig. 1A). At higher H_2O , the calibrations become non-linear and the three compositional groups begin to deviate from one another; a similar deviation for basalt was observed by Sobolev and Chaussidon (1996) using different analytical conditions. The CO_2 calibrations for basalt and andesite are identical, while the rhyolite CO_2 calibration shows a steeper slope (Fig. 1B). The other calibration curves (F, S, Cl) are linear over several orders of magnitude in volatile concentration for all glasses, with no differences among the three groups of standards. The calibration curves are all constrained by a large number of samples of varying composition. For F, S and Cl, the measured isotope ratios ($^{19}\text{F}/^{30}\text{Si}$, $^{32}\text{S}/^{30}\text{Si}$, $^{35}\text{Cl}/^{30}\text{Si}$) are normalized to a SiO_2 content of 50 wt.% (e.g. multiplied by the ratio [wt.% $\text{SiO}_2/50$]) and then regressed against the standard concentrations (from FTIR, manometry, and/or electron probe data). A linear regression is made in log–log space so that high-concentration standards do

Fig. 1. SIMS calibration curves for abundances of (A) water, (B) carbon dioxide, (C) fluorine, (E) sulfur and (F) chlorine. Panel (D) shows the SIMS matrix effect on the CO_2 calibration, correlated with Na and Ca concentrations of the standard glasses. The H_2O calibrations for basalt, andesite and rhyolite are identical below 1.5 wt.% H_2O , but deviate and become non-linear at higher H_2O . The other calibrations are linear over several orders of magnitude in concentration. Detection limits are 10–30 ppm H_2O , < 3 ppm CO_2 , and < 1 ppm for F, S and Cl. Solid circles are basalts, solid triangles are andesites, and open circles are rhyolites.



not dominate the slope of the calibration line, and the calibrations are linear (in linear–linear space) within error. The scatter of standards about the calibration lines is the best estimate of accuracy, and averages 10% for all elements.

Most previous efforts at SIMS calibrations for volatile elements have involved the use of a beam O^- ions and measurement of positively charged sputtered ions (Hervig, 1992; Sisson and Layne, 1993; Ihinger et al., 1994; Devine et al., 1995; Deloule et al., 1995; Sobolev and Chaussidon, 1996). This strategy has the advantage of simplified charge compensation, but the disadvantage of low sensitivity for electronegative elements such as C, F, S and Cl and correspondingly poor detection limits. Improvements in electron charge compensation have permitted the development of the present technique, and our efforts have focussed on analysis of a large number of compositionally diverse standard glasses. Matrix effects were searched for by calculating slopes for tie lines between each standard and the origin, and plotting the slopes against various compositional parameters. The calibrations for F, S and Cl are free of significant matrix effects, but the H_2O and CO_2 abundance calibrations have resolvable matrix effects which deserve further mention.

4.1. Water

For our technique, the best correlative for water matrix effects is the H_2O content of the standard. Ion yields for both H and Si decrease with increasing water content. The water calibrations for basalt, andesite and rhyolite are identical below 1.5 wt.% H_2O , but become increasingly different at higher water contents (Fig. 1A). The average scatter of standards about the calibration line is 12%, but the comparison between FTIR and SIMS on the same polished wafers is better at 8%, comparable to the accuracy of the FTIR method alone. We consider the accuracy of the SIMS calibration for water to be accurate to 10% for compositions ranging from nephelenite through andesite to rhyolite.

Another feature we have noted about the H_2O calibration is that the slope of the calibration line has been observed to change by as much as a factor of two between analytical sessions, while preserving the relative positions of all the standards along the cali-

bration line. These changes in slope are unique to the H_2O calibration, and are related to two factors: (1) the quality of electron gun tuning and corresponding homogeneity in charge compensation, and (2) the quantum efficiency (number of secondary electrons per incident ion) of the electron multiplier for H ions, which is a sensitive function of multiplier high voltage and age. In the Cameca 6f instrument, the stray magnetic field originating from the mass spectrometer magnet is sufficiently strong to deflect the electron beam by 20 μm when switching between mass 1 (H) and mass 35 (Cl), and this has been mediated during analysis by including a shift in the electron beam deflection which is correlated with mass. For the electron multiplier, the efficiency is routinely measured by comparing count rates on the multiplier and Faraday cup detectors. If the multiplier efficiency for ^{28}Si is kept near 90% (by adjusting multiplier high voltage), then changes in the H_2O calibration slope are minimized. To check these effects, at the beginning of each analytical session, the H_2O calibration is always redetermined and standards are run frequently to make sure that the calibration does not drift during a single analytical session.

4.2. Carbon

For our technique, the best correlative for CO_2 matrix effects is the ratio of $Na_2O/(Na_2O + CaO)$, as has been observed for FTIR absorbance measurements (Dixon and Pan, 1995). This matrix effect is resolvable even among the basaltic glasses (nephelenite through tholeiite) (Fig. 1F). The CO_2 calibration is thus constructed by regressing standard concentrations against SiO_2 -normalized $^{12}C/^{30}Si$ ratios, the slopes of which are then adjusted according to the ratio of $Na_2O/(Na_2O + CaO)$. The resulting calibration is linear over almost four orders of magnitude in CO_2 abundance, with an accuracy (15%) which is comparable to the accuracy of FTIR measurements.

4.3. Fluorine, sulfur and chlorine

The main advantage of ion probe measurements of F, S and Cl over electron probe methods is in the signal-to-background ratio. Typical background measurements on the ion probe are on the order of 0.05–0.1 counts per second, compared to tens to hundreds

of counts per second for the electron probe. In particular, F analyses in Fe-bearing materials suffer from interferences from Fe X-rays, making electron probe F analysis of basaltic and andesitic glasses difficult. For the SIMS methods, hundreds of counts on ^{19}F , ^{32}S and ^{35}Cl are obtained even for measurements of detection limits on San Carlos olivine, with corresponding signal-to-background ratios of >1000 in olivine which is nominally free of F, S and Cl. As a result, ion probe detection limits are better and analysis times shorter for these elements compared with existing electron probe methods.

5. Isotopic measurements: hydrogen, carbon, and sulfur

Hydrogen and carbon isotope analysis of low- H_2O and low- CO_2 glasses requires careful attention to background effects. Despite careful cleaning of glass surfaces with teflon-distilled water and subsequent drying of samples in an oven, hydrogen and carbon contamination of the sample surface is ubiquitous and unavoidable. Although this surface layer is usually sputtered through in a matter of seconds, the intersection of this layer with the wall of the sputter crater is a site of continuous formation of contaminant ions. For both measurements, particular attention must be paid to centering of the field aperture in the sharply focused image of the sputter crater, so that ion contributions from the crater walls are entirely eliminated. Backgrounds for H and C are usually determined by sputtering of San Carlos olivine, which is thought to have nominal concentrations of 10 ppm H_2O and <1 ppm CO_2 . Typical count rates are $1\text{--}2 \times 10^4$ cps ^1H and $2\text{--}5$ cps ^{12}C , with a measured D/H ratio which is typically within 50–80‰ of D/H ratios measured in standard glasses. We consider these counts to be dominated by H (and perhaps C) atoms which are actually present in the olivine crystal, because San Carlos olivine often plots close to the basalt calibration curve. As a result, the true instrumental backgrounds are difficult to quantify, but are routinely $<10\text{--}30$ ppm H_2O and <2 ppm CO_2 , and insignificant for isotopic measurements.

Typically, a 40- μm diameter primary beam is used. The 400- μm field aperture images a circular area 20 μm in diameter on the sample surface and thereby

masks ions from the outer 10 μm of the crater. Obtaining a sharp ion image of the sputter crater is essential for this application, and can be complicated by the electron gun used for charge compensation. When the electron current is too high, the electrostatic field established by the presence of the electron beam in the secondary ion path results in an ion image which is degraded. In addition, if the high voltage setting of the electron beam is not matched perfectly with the sample voltage, electrons can impact the sample and produce desorbed H^- ions (Hervig et al., 1992). For these reasons, the electron beam current is kept to a level twice that which is required for charge compensation of a 20–40 nA Cs^+ beam.

SIMS hydrogen isotope measurements of basalt, andesite and rhyolite glasses are shown in Fig. 2A. The value of the instrumental mass fractionation (IMF) factor α ($\alpha = \text{D}/\text{H}_{\text{measured}}/\text{D}/\text{H}_{\text{true}}$) is a complex function of sample composition, as found for amphiboles under different analytical conditions (Delouie et al., 1991), but H_2O and Fe content are two important correlatives. For example, IMF is negatively correlated with H_2O content in all three glass compositions (basalt, andesite, rhyolite) but is positively correlated with Fe content in glasses with similar H_2O abundances. Basalts with <1 wt.% H_2O all show similar IMF values (Fig. 2A), but rhyolite IMF is a function of H_2O content in this range. The absolute values of α vary between analysis sessions, driven by changes related to quantum efficiency and aging of the electron multiplier, but the relative differences in IMF among different standards are constant. A more detailed consideration of D/H matrix effects will be presented elsewhere (Hauri et al., in preparation).

Carbon isotope data for the natural (406 ppm CO_2) and synthetic (7000 ppm CO_2) basalts give the same IMF to better than 1‰, and also give IMF values that are larger than the andesite glasses (Fig. 2B). Carbon isotope data for MORB glasses and three Loihi melt inclusions are shown in Fig. 2C. Several factors conspire to limit the precision and reproducibility of $\delta^{13}\text{C}$ analyses of CO_2 -bearing glasses to about 2–3‰, not the least of which is the low abundance of the element of interest. The requirement of high mass resolution places limits on the size of the field aperture used, charge compensation considerations limit the intensity of the primary beam to <50 nA, and control over instrumental mass fractionation pla-

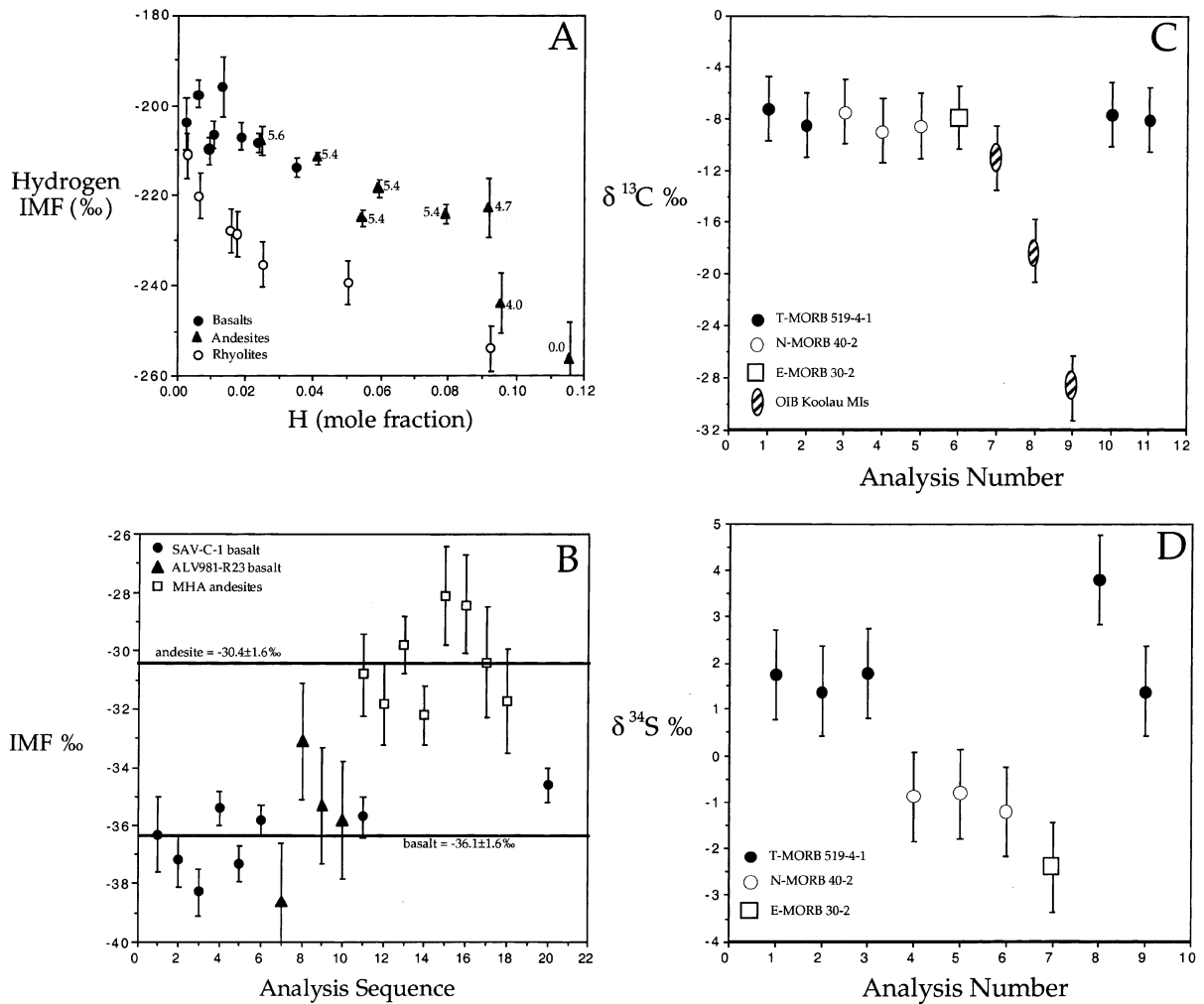


Fig. 2. (A) Instrumental mass fractionation (IMF) factors for D/H measurements in silicate glasses (given as the permil deviation of the measured D/H ratio from the true D/H ratio) against mole fraction of water in the standards. IMF measurements on any single standard are usually reproducible to ± 3 permil (1σ), but some glasses show subtle heterogeneity. Significant matrix effects are apparent, as IMF is strongly correlated with H_2O content within each group of glasses. Small numbers beside andesite points (triangles) give the total FeO content. (B) IMF factors for analysis of carbon isotopes in silicate glasses. Two basalt standards give the same IMF value to within 2‰, but the basalts are more fractionated than the andesites by about 6‰. No variation of carbon isotope IMF is apparent within the andesites (1.09–3.70 wt.% H_2O). (C) Carbon isotope data for several MORB H_2O standards and three basaltic melt inclusions from Koolau volcano, Hawaii. (D) Sulfur isotope data for MORB H_2O glass standards, showing resolvable S isotope variability.

ces limits on the depth of the sputter crater ($< 50\%$ of the beam diameter). However, an advantage of SIMS over vacuum combustion for $\delta^{13}\text{C}$ analyses is the ability to access directly carbon dissolved in the silicate glass, thus avoiding problems related to adsorption, carbonate or seawater alteration and organic contamination (Mattey et al., 1984), CO_2

gas in micro-vesicles (Pineau and Javoy, 1983), and precipitation of reduced C phases on vesicle walls (Mathez and Delaney, 1981).

For $\delta^{34}\text{S}$ analyses in basaltic glasses, the instrumental mass fractionation factor α is relatively reproducible at 0.990 ± 0.003 ; this value is strictly applicable only to relatively low- H_2O (< 1 wt.%) basaltic

glasses similar to the ALV 519-4-1 standard. This α value is different from that measured in our lab on Fe–Ni–Cu sulfide standards at high mass resolution (0.96–0.98). Sulfur ion counts for basaltic glasses (usually >700 ppm S) are sufficiently high that a count rate of 10×10^6 cps on ^{32}S is easily attainable, producing an in-run precision of 0.3‰ in 30 min. However, reproducibility is typically worse at 1–2‰ (Fig. 2D). Sample heterogeneity may be one explanation for this observation, particularly if tiny immiscible sulfides (occasionally observed in ion images) with α values different from glass are sputtered during analysis. An equally likely explanation for this poor reproducibility relates to the fact that small changes in the primary beam position within the secondary ion optical image field result in subtle changes in the position of the ion optic crossover relative to the entrance slits, which are closed slightly to achieve the required mass resolution. Since the crossover is known to be isotopically heterogeneous in Cameca ion probes (Shimizu and Hart, 1982), these small changes in beam position may contribute to errors at the 1–2‰ level. Such problems are absent in techniques which transmit the entire crossover, such as for S isotope analyses on sulfides using energy filtering at low mass resolution (Riciputi, 1996), or techniques utilizing a mass spectrometer with an intrinsically high minimum mass resolving power such as the Cameca 1270 or SHRIMP.

6. Applications

In its current state of development, we regard the SIMS techniques for measuring volatiles as being superior to existing electron probe methods, and complementary to current FTIR methods. Infrared spectroscopy provides important quantitative information on volatile speciation which is not obtainable by SIMS, and this information is critical to studies of stable isotope fractionation of volatile species (Taylor, 1988), low-temperature alteration (Dixon et al., 1997), and for understanding diffusion (Zhang and Stolper, 1991). With sufficient absorbance, FTIR techniques also may provide a better detection limit for H_2O than SIMS, making possible the analysis of nominally anhydrous minerals (Bell and Rossman, 1992), but SIMS calibration efforts for such minerals are begin-

ning to improve (Koga et al., unpublished data). The SIMS technique offers ease of sample preparation, adequate detection limits for most studies, and the capability to obtain stable isotope data for hydrogen and, if present in sufficient quantity, carbon and sulfur. Both techniques offer the advantages of rapid analysis and micron-scale spatial resolution.

The techniques described above have obvious utility in studies of volatile degassing during volcanic eruptions. Fig. 3 shows the H_2O and δD data obtained by SIMS for the four Mono Craters rhyolite standards, compared with FTIR data for H_2O and gas-source mass spectrometry data on bulk glass separates reported by Newman et al. (1988). Except for the previously mentioned discrepancy for the H_2O content of our North Coulee glass sample (not plotted), the two data sets show good agreement. Combined with FTIR data on hydrogen speciation in these glasses, the data fit well the model of Newman et al. (1988) in which the vapor-melt D/H fractionation factor changes with water content and H-speciation. Similar H_2O and δD measurements can be obtained on melt inclusions contained in phenocrysts from

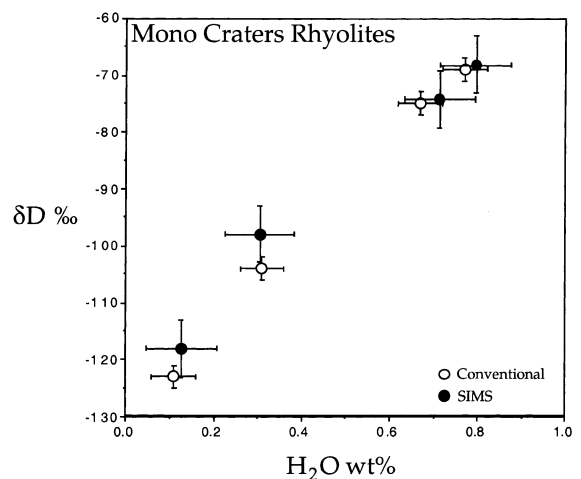


Fig. 3. H_2O and δD data for Mono Craters rhyolite glasses, comparing data obtained by conventional vacuum extraction mass spectrometry (open symbols, Newman et al., 1988) and data obtained by SIMS (closed symbols, this study). The SIMS H_2O and δD data were corrected for matrix effects using calibrations constrained by all standards. SIMS data were obtained on separate fragments from the same hand specimens used for the vacuum extractions, and the results show good agreement.

silicic eruptions; when combined with CO₂ measurements, such data have the potential to provide important information on volatile zonation of silicic magma chambers prior to eruption (Wallace et al., 1995).

Carbon isotope data are shown in Fig. 2C for several MORB glass H₂O standards. Data for $\delta^{13}\text{C}$ in the MORB glasses cluster around a value of $-8.0 \pm 3\text{‰}$, close to the proposed mantle value of -5‰ (Pineau and Javoy, 1983; Matthey et al., 1984). Three melt inclusions from a Koolau (Hawaii) basalt, however, show variable depletion in ^{13}C reaching values of $\delta^{13}\text{C}$ of -29‰ . Due to the mass fractionation between dissolved carbonate and CO₂ vapor at magmatic temperatures, these very depleted $\delta^{13}\text{C}$ values could have been generated by open-system CO₂ loss, but the slope of the trend with CO₂ content is too shallow for degassing with a 4‰ fractionation between CO₂ vapor and dissolved carbonate (Javoy et al., 1978). An additional possibility is mixing between highly degassed and undegassed magma batches (Dixon et al., 1991), but the generally moderate CO₂ contents of these melt inclusions (250–550 ppm) would require initial CO₂ contents of several thousand parts per million to reach a $\delta^{13}\text{C}$ value of -5‰ . Although these postulated CO₂ abundances are high, they are consistent with several similar determinations (Pineau and Javoy, 1983; Des Marais and Moore, 1984; Greenland et al., 1985; Gerlach and Graeber, 1985). The isotopically depleted CO₂ contained within melt inclusions demonstrate conclusively the presence of isotopically depleted carbon dissolved in the glass, and suggests that magmatic degassing could be capable of producing large C isotope shifts. Thus the origin of very low $\delta^{13}\text{C}$ values in volcanic glasses are not uniquely explained by organic carbon contamination (Matthey et al., 1984) or by late-stage precipitation of carbonaceous phases within vesicles (Mathez and Delaney, 1981).

Isotope data for some volatile elements may also provide information on magma source compositions. Fig. 2D shows sulfur isotope data for three of our MORB glass H₂O standards. Sample 40-2 is a strongly LREE-depleted N-type MORB glass, sample 30-2 is a LREE-enriched E-type MORB, and 519-4-1 is transitional. There are resolvable isotopic differences between these three samples. Because the

samples were erupted at >1000 m depth on the seafloor and are H₂O-undersaturated, it is very unlikely that they have degassed significant amounts of sulfur. Possibilities to explain the data include high-temperature S isotope fractionations during melting or segregation of immiscible sulfides, assimilation of seawater sulfate in the crust, or mantle heterogeneity.

7. Conclusions

This report demonstrates the advantages of SIMS in sensitivity, rapidity and detection limits over other microbeam methods for analysis of volatiles in silicate glasses. Indeed, the sensitivity is sufficiently high to permit useful isotopic measurement of H, C and S dissolved in quenched silicate melts. This technique is applicable to the study of submarine and subaerial volcanic glasses as well as laboratory melting experiments. The study of volatile abundances in phenocryst-hosted melt inclusions is one area where the strengths of the SIMS volatile techniques become highly advantageous. Though many IR studies of melt inclusions have been reported (e.g. Anderson and Brown, 1993; Clague et al., 1996; Wallace and Anderson, 1998), preparation of doubly polished wafers of small inclusions is time-consuming and difficult, and the polished inclusions must be thick enough to permit accurate absorbance measurements. These factors mitigate against analyzing large numbers of inclusions, and introduces a potential bias against small inclusions. Melt inclusions down to 10–15 μm in diameter can be analyzed for volatile abundances by SIMS, and the use of singly polished grain mounts makes possible the rapid preparation of a large number of inclusions. In particular, the SIMS techniques described here offer the possibility of obtaining isotopic information for H, C and S in melt inclusions when these elements are present in sufficient quantities. When applied to melt inclusions from Hawaii (Hauri, 2001), combined data for volatile abundances and isotopic compositions reveal several processes which influence magmatic volatile contents. Indeed, several of these processes would escape detection altogether in the absence of a complete volatile dataset.

Acknowledgements

We thank Alex Sobolev for providing MORB glasses 30-2 and 40-2, Rick Hervig for loans of ion probe mounts and illuminating discussions, Richard Kingsley and Bruce Taylor for D/H measurements, and Dave Virgo for uncovering and donating a number of H₂O-bearing glasses from the olden days. Thanks also to Colin Macpherson and David Hilton for providing sample ALV981-R23 as a C isotope standard, and Jean Guy-Schilling and Richard Kingsley for basalt glasses from the Pacific Ocean. Acquisition of the DTM ion microprobe was made possible by funds from NSF, the Carnegie Institution of Washington, the W.M. Keck Foundation, the Smithsonian Institution, the USGS and Dr. Robert Golet. The paper was improved by thorough reviews from John Eiler, Marc Chaussidon and Paul Wallace. This work was supported by NSF grants EAR-9413985 and OCE-9712278 to EHH.

References

- Anderson, A.T., Brown, G.G., 1993. CO₂ and formation pressures of some Kilauea melt inclusions. *Am. Mineral.* 78, 794–803.
- Bell, D.R., Rossman, G.R., 1992. Water in the Earth's mantle: the role of nominally anhydrous minerals. *Science* 255, 1391–1397.
- Byers, C.D., Garcia, M.O., Muenow, D.W., 1985. Volatiles in pillow rim glasses from Loihi and Kilauea volcanoes, Hawaii. *Geochim. Cosmochim. Acta* 49, 1887–1896.
- Clague, D.A., Moore, J.G., Dixon, J.E., Friesen, W.B., 1996. Petrology of submarine lavas from Kilauea's Puna Ridge, Hawaii. *J. Petrol.* 36, 299–349.
- Delaney, J.R., Karsten, J.L., 1981. Ion microprobe studies of water in silicate melts: concentration dependent water diffusion in obsidian. *Earth Planet. Sci. Lett.* 52, 191–202.
- Deloule, E., France-Lanord, C., Albarede, F., 1991. D/H analysis of minerals by ion probe. In: Taylor, H.P., O'Neil, J., Kaplan, I.R. (Eds.), *Stable Isotope Geochemistry: A Tribute to Samuel Epstein*. Geochemical Society, Special Publication, vol. 3, 53–62.
- Deloule, E., Paillat, O., Pichavant, M., Scaillet, B., 1995. Ion microprobe determination of water in silicate glasses: methods and applications. *Chem. Geol.* 125, 19–28.
- Des Marais, D.J., Moore, J.G., 1984. Carbon and its isotopes in mid-oceanic basaltic glasses. *Earth Planet. Sci. Lett.* 69, 43–57.
- Devine, J.D., Gardner, J.E., Brack, H.P., Layne, G.D., Rutherford, M.J., 1995. Comparison of microanalytical methods for estimating H₂O contents of silicic volcanic glasses. *Am. Mineral.* 80, 319–328.
- Dixon, J.E., Clague, D.A., 2001. Volatiles in basaltic glasses from Loihi Seamount, Hawaii: evidence for a relatively dry plume component. *J. Petrol.* 42, 627–654.
- Dixon, J.E., Pan, V., 1995. Determination of the molar absorptivity of dissolved carbonate in basaltic glass. *Am. Mineral.* 80, 1339–1342.
- Dixon, J.E., Stolper, E.M., 1995. An experimental study of water and carbon dioxide solubilities in mid-ocean ridge basaltic liquids: Part II. Applications to degassing. *J. Petrol.* 36, 1633–1646.
- Dixon, J.E., Stolper, E., Delaney, J.R., 1988. Infrared spectroscopic measurements of CO₂ and H₂O in Juan de Fuca Ridge basaltic glasses. *Earth Planet. Sci. Lett.* 90, 87–104.
- Dixon, J.E., Clague, D.A., Stolper, E.M., 1991. Degassing history of water, sulfur and carbon in submarine lavas from Kilauea volcano, Hawaii. *J. Geol.* 99, 371–394.
- Dixon, J.E., Clague, D.A., Wallace, P., Poreda, R., 1997. Volatiles in alkalic basalts from the North Arch volcanic field, Hawaii: extensive degassing of deep submarine-erupted alkalic series lavas. *J. Petrol.* 38, 911–939.
- Fine, G., Stolper, E.M., 1985. The speciation of carbon dioxide in sodium aluminosilicate glasses. *Contrib. Mineral. Petrol.* 91, 105–121.
- Fine, G., Stolper, E.M., 1986. Dissolved carbon dioxide in basaltic glasses: concentration and speciation. *Earth Planet. Sci. Lett.* 76, 263–278.
- Fogel, R.A., 1989. The role of H–C–O–S volatile in planetary igneous processes. PhD Thesis, Brown University, Providence, RI.
- Fogel, R.A., Rutherford, M.J., 1990. The solubility of carbon dioxide in rhyolitic melts: a quantitative FTIR study. *Am. Mineral.* 75, 1311–1326.
- Garcia, M.O., Muenow, D.W., Aggrey, K.E., O'Neil, J.R., 1989. Major element, volatile and stable isotope geochemistry of Hawaiian submarine tholeiitic glasses. *J. Geophys. Res.* 94, 10525–10538.
- Gerlach, T.M., Graeber, E.J., 1985. Volatile budget of Kilauea volcano. *Nature* 313, 273–277.
- Greenland, L.P., Rose, W.I., Stokes, J.B., 1985. An estimate of gas emissions and magmatic gas content from Kilauea volcano. *Geochim. Cosmochim. Acta* 49, 125–129.
- Grzechnik, A., Zimmermann, H.D., Hervig, R.L., King, P.L., McMillan, P.F., 1996. FTIR micro-reflectance measurements of the CO₃²⁻ ion content in basaltic and leucite glasses. *Contrib. Mineral. Petrol.* 125, 311–318.
- Hauri, E.H., 2002. SIMS investigations of volatiles in volcanic glasses, 2: isotopes and abundances in Hawaiian melt inclusions. *Chem. Geol.*
- Hauri, E.H., Wang, J., Dixon, J.E., King, P., Mandeville, C., Newman, S., 2002. Sputtering and matrix effects during SIMS analysis of hydrogen isotopes in silicate glasses. *Chem. Geol.* (in preparation).
- Hervig, R.L., 1992. Ion probe microanalyses for volatile elements in melt inclusions (abst.). *EOS Trans. Am. Geophys. Union* 73, 367.
- Hervig, R.L., Williams, P., Thomas, R.M., Schauer, S.N., Steele, I.M., 1992. Microanalysis of oxygen isotopes in insulators by secondary ion mass spectrometry. *Int. J. Mass Spectrom. Ion Proc.* 120, 45–63.

- Hinthorne, J.R., Anderson, C.A., 1975. Microanalysis of fluorine and hydrogen in silicates with the ion microprobe mass analyzer. *Am. Mineral.* 60, 143–147.
- Hoskin, P.W.O., 1999. SIMS determination of $\mu\text{g/g}$ -level fluorine in geological samples and its concentration in NIST SRM 610. *Geostand. Newsl.* 23, 69–76.
- Ihinger, P., Hervig, R.L., McMillan, P.F., 1994. Analytical methods for volatiles in glasses. In: Valley, J.W., Taylor, H.P., O'Neil, J.R. (Eds.), *Stable Isotopes in High Temperature Geologic Processes*. Mineralogical Society of America, Chelsea, MI, pp. 67–121.
- Javoy, M., Pineau, F., Iiyama, I., 1978. Experimental determination of the isotopic fractionation between gaseous CO_2 and carbon dissolved in tholeiitic magma. *Contrib. Mineral. Petrol.* 67, 35–39.
- King, P.L., 1999. C–O–H Volatiles in Igneous Rocks: Experimental and Natural Studies of Hydrous Minerals and Glasses. PhD thesis, Arizona State University, Tempe, AZ.
- Macpherson, C.G., Hilton, D.R., Newman, S., Matthey, D.P., 1999. CO_2 , $^{13}\text{C}/^{12}\text{C}$ and H_2O variability in natural basalt glasses: a study comparing stepped heating and FTIR spectroscopic techniques. *Geochim. Cosmochim. Acta* 63, 1805–1813.
- Mathez, E.A., Delaney, J.R., 1981. The nature of carbon in submarine basalts and peridotite nodules. *Earth Planet. Sci. Lett.* 56, 217–232.
- Matthey, D.P., Carr, R.C., Wright, I.P., Pillinger, C.T., 1984. Carbon isotopes in submarine basalts. *Earth Planet. Sci. Lett.* 70, 196–206.
- Mackwell, S.J., Kohlstedt, D.L., 1990. Diffusion of hydrogen in olivine: implications for water in the mantle. *J. Geophys. Res.* 95, 5079–5088.
- Michael, P., 1995. Regionally distinctive sources of depleted MORB: evidence from trace elements and H_2O . *Earth Planet. Sci. Lett.* 131, 301–320.
- Newman, S., Stolper, E.M., Stolper, E., 1986. Measurement of water in rhyolitic glasses: calibration of an infrared spectroscopic technique. *Am. Miner.* 71, 1527–1541.
- Newman, S., Epstein, S., Stolper, E., 1988. Water, carbon dioxide, and hydrogen isotopes in glasses from the ca. 1340 A.D. eruption of the Mono craters, California: constraints on degassing phenomena and initial volatile content. *J. Volcanol. Geotherm. Res.* 35, 75–96.
- Pineau, F., Javoy, M., 1983. Carbon isotopes and concentrations in mid-ocean ridge basalts. *Earth Planet. Sci. Lett.* 62, 239–257.
- Riciputi, L.R., 1996. A comparison of extreme energy filtering and high mass resolution techniques for the measurement of $^{34}\text{S}/^{32}\text{S}$ ratios by ion microprobe. *Rapid Commun. Mass Spectrom.* 10, 282–286.
- Rison, W., Craig, H., 1983. Helium isotopes and mantle volatiles in Loihi seamount and Hawaiian Island basalts and xenoliths. *Earth Planet. Sci. Lett.* 66, 407–426.
- Shimizu, N., Hart, S.R., 1982. Applications of the ion microprobe to geochemistry and cosmochemistry. *Annu. Rev. Earth Planet. Sci.* 10, 483–526.
- Silver, L.A., Ihinger, P.D., Stolper, E.M., 1990. The influence of bulk composition on the speciation of water in silicate glasses. *Contrib. Mineral. Petrol.* 104, 142–162.
- Sisson, T.W., Layne, G.D., 1993. H_2O in basalt and basaltic andesite glass inclusions from four subduction-related volcanoes. *Earth Planet. Sci. Lett.* 117, 619–635.
- Sobolev, A.V., Chaussidon, M., 1996. H_2O concentrations in primary melts from supra-subduction zones and mid-ocean ridges: implications for H_2O storage and recycling in the mantle. *Earth Planet. Sci. Lett.* 137, 45–55.
- Stolper, E., 1982. Water in silicate glasses: an infrared spectroscopic study. *Contrib. Mineral. Petrol.* 81, 1–17.
- Stolper, E.M., Holloway, J.R., 1988. Experimental determination of the solubility of carbon dioxide in molten basalt at low pressure. *Earth Planet. Sci. Lett.* 87, 397–408.
- Stolper, E.M., Newman, S., 1994. The role of water in the petrogenesis of Mariana Trough magmas. *Earth Planet. Sci. Lett.* 121, 293–325.
- Taylor, B.E., 1988. Magmatic volatiles: isotopic variation of H, C and S. In: Valley, J.W., Taylor, H.P., O'Neil, J.R. (Eds.), *Stable Isotopes in High Temperature Geologic Processes*. Mineralogical Society of America, Chelsea, MI, pp. 185–225.
- Wallace, P.J., Anderson, A.T., 1998. Effects of eruption and lava drainback on the H_2O contents of basaltic magmas at Kilauea volcano. *Bull. Volcanol.* 59, 327–344.
- Wallace, P.J., Wallace Jr., A.T.A., Davis, A.M. 1995. Quantification of pre-eruptive exsolved gas contents in silicic magmas. *Nature* 377, 612–616.
- Zhang, Y., Stolper, E.M., 1991. Water diffusion in a basaltic melt. *Nature* 351, 306–309.
- Zhang, Y., Belcher, R., Ihinger, P.D., Wang, L., Xu, Z., Newman, S., 1997. New calibration of infrared measurement of dissolved water in rhyolitic glasses. *Geochim. Cosmochim. Acta* 61, 3089–3100.